Autonomous Self-healing and Superior Tough Polyurethane Elastomers Enabled by Strong and Highly Dynamic Hard Domains

Hao Jiang[a], Tong Yan[a], Meng Cheng[a, b], Zhihao Zhao[a], Tinglei He[a], Zhikun Wang[a, b], Chunling Li[a, b*], Shuangqing Sun[a, b*], Songqing Hu[a, b]

a School of Materials Science and Engineering, China University of Petroleum (East China), Qingdao 266580, China.

b Institute of Advanced Materials, China University of Petroleum (East China), Qingdao 266580, China.

**Corresponding authors: Shuangqing Sun (sunshuangqing@upc.edu.cn), Chunling Li (lichunling@upc.edu.cn)*

Experimental Methods

Materials

Hexane (98%), dibutyltin dilaurate (99%, DBTDL), acetone (99.8%), ethanol (99.8%), $CHCl_3$ (99.8%) and N, N-Dimethylacetamide (99.8%, DMAc) were obtained from Sinopharm. Polytetramethylene ether glycol (PTMEG, Mn=1000 $g \cdot mol^{-1}$), isophorone diisocyanate (99%, IPDI), phenylamine (99.85%), 2-Amino-2-methyl-1.3-propanediol (98%, AMPD) were obtained from Aladdin Chemistry (Shanghai) Co., Ltd. Hexamethylene diisocyanate (99%, HDI) was obtained from Shanghai Macklin Biochemical Co., Ltd. Deionized water (18 MΩ cm) was used during the whole experiments.

Synthesis of 1-(6-isocyanatohexyl)-3-phenylurea (HU_2-NCO)

HDI (10.09 g, 60 mmol) was added into a three-necked glass flask and then the flask was purged with N_2. Subsequently, phenylamine (1.12 g, 12 mmol) was injected into flask with vigorous stirring. The reaction was carried out at 25 °C for 24 h under a N_2 atmosphere. Subsequently, the reaction mixture was washed extensively with hexane to remove unreacted HDI. The resulting white powder, HU_2-NCO, was obtained after drying the product at 40 °C for 12 h (2.88 g, yield, 92%). ^{1}H NMR (400 MHz, DMSO-d6): δ 8.38 (s, 1H), 7.37 (d, J = 8.0 Hz, 2H), 7.21 (t, J = 7.9 Hz, 2H), 6.87 (t, J = 7.3 Hz, 1H), 6.11 (d, J = 5.2 Hz, 1H), 3.07 (q, J = 6.4 Hz, 2H), 2.95 (s, 2H), 1.76-0.89 (m, 8H).

Synthesis of 1-(6-(3-(1,3-dihydroxy-2-methylpropan-2-yl)ureido)hexyl)-3-phenylurea (HU_2-OH)

HU_2-NCO (2.61 g, 10 mmol) and AMPD (1.36 g, 12.95 mmol) were mixed in dried $CHCl_3$. The mixture was stirred at 60 °C for 10 h under a N_2 atmosphere. After the

reaction, the mixture was filtrated and washed with $CHCl_3$ and then dissolved in 120 mL of acetone. The resulting cloudy solution was centrifuged to acquire the white solid. After the residual acetone was removed at 50 °C overnight, the white powder was dissolved in 120 mL of ethanol and then centrifuged to obtain the supernatant liquid. Subsequently, the liquid was mixed with excess water, filtered and dried to obtain HU_2-OH. ^{1}H NMR (400 MHz, DMSO-d6): δ 8.35 (s, 1H), 7.45-7.29 (d, 2H), 7.29-7.13 (t, 2H), 6.87 (t, J = 7.3 Hz, 1H), 6.16 (t, J = 5.4 Hz, 1H), 6.09 (t, J = 5.5 Hz, 1H), 5.62 (d, J = 6.6 Hz, 2H), 5.09 (t, J = 5.5 Hz, 1H), 3.40 (dd, J = 10.6, 5.4 Hz, 2H), 3.33 (d, J = 5.7 Hz, 2H), 3.07 (d, J = 6.5, 5.5 Hz, 2H), 2.94 (d, J = 6.4 Hz, 2H), 1.51-1.18 (m, 8H), 1.08 (s, 3H).

Synthesis of 1-(3-(isocyanatomethyl)-3,5,5-trimethylcyclohexyl)-3-phenylurea and 1-((5-isocyanato-1,3,3-trimethylcyclohexyl)methyl)-3-phenylurea (IPU_2-NCO)

IPDI (13.32 g, 60 mmol) was added into a three-necked glass flask, and then the flask was then purged with N_2. Subsequently, phenylamine (1.12 g, 12 mmol) was injected into flask with vigorous stirring. The mixture was reacted at 40 °C for 48 h under a N_2 environment. After the reaction, the solution was slowly dropped into excess hexane under vigorously stirring and allowed to stand for 2 h. The lower layer of viscous liquid was then collected and placed at 40 °C overnight under vacuum to obtain IPU_2-NCO. ^{1}H NMR (400 MHz, DMSO-d6): δ 8.35 (s, 1H), 8.27 (s, 1H), 7.45-7.32 (m, 4H), 7.21 (d, J = 7.8 Hz, 4H), 6.88 (t, J = 7.2 Hz, 2H), 6.23 (t, J = 6.2 Hz, 1H), 5.96 (dd, J = 19.9, 7.7 Hz, 1H), 3.84 (m, 1H), 3.78-3.28 (m, 4H), 2.87 (d, J = 4.8 Hz, 1H), 1.95-1.49 (m, 8H), 1.32-0.72 (m, 22H).

Synthesis of 1-(3-((3-(1,3-dihydroxy-2-methylpropan-2-yl)ureido)methyl)-3,5,5-trimethylcyclohexyl)-3-phenylurea and 1-((5-(3-(1,3-dihydroxy-2-methylpropan-2-yl)ureido)-1,3,3-trimethylcyclohexyl)methyl)-3-phenylurea (IPU_2-OH)

IPU_2-NCO (3.15 g, 10 mmol) and AMPD (1.36 g, 12.95 mmol) were mixed in dried acetone and reacted at 60 °C for 10 h. After the reaction, the mixture was mixed with excess water, filtered and dried to obtain IPU_2-OH. ^{1}H NMR (400 MHz, DMSO-d6): δ 8.36 (s, 1H), 8.27 (s, 1H), 7.46-7.29 (m, 4H), 7.29-7.13 (m, 4H), 6.87 (t, J = 7.2 Hz, 2H), 6.22 (d, J = 24.1 Hz, 1H), 6.05 (d, J = 7.8 Hz, 1H), 5.98-5.82 (m, 2H), 5.77 (s, 1H), 5.56 (s, 1H), 5.10 (q, J = 5.1 Hz, 4H), 3.99-3.53 (m, 2H), 3.40 (dd, J = 10.4, 4.9 Hz, 8H), 2.97-2.63 (m, 4H), 1.78-1.28 (m, 14H), 1.28-0.62 (m, 22H).

Preparation of PU-HU_2-n (or PU-IPU_2-n) elastomers

Before the reaction, PTMEG was added into a 100 mL glass flask and then heated at 120 °C for 2 h under vacuum to remove residual moisture. Subsequently, a solution containing 3 mL of DMAc, IPDI (0.445g, 2 mmol), one drop of DBTDL and an appropriate amount of PTMEG was prepared and injected into a three-necked glass flask. The mixture was reacted at 60 °C for 3.5 h under a N_2 atmosphere. Afterward, a precise amount of HU_2-OH (or IPU_2-OH) was dissolved in 3 mL of DMAc and added to the flask. The mixture was then stirred for another 3.5 h at 80 °C to obtain the PU-HU_2-n (or PU-IPU_2-n) solution. The symbol "n" represent the molar percentage of HU_2-OH (or IPU_2-OH) calculated using the following equation:

$$n\% = \frac{n(HU_2\text{-}OH)}{n(IPDI)} \times 100\% \#(1)$$

Here, n(HU_2-OH), and n(IPDI) represent the molar quantities of HU_2-OH and IPDI, respectively. The stoichiometric ratio of -NCO and -OH groups was maintained at 1:1. The resulting solution was initially poured into a PTFE mold groove measuring 25 × 5 × 1 mm^3. Subsequently, it was heated at 60 °C under vacuum for 5 min to eliminate any residual bubbles. Following this, the product was dried at 60 °C for 48 h, followed by an additional 24 h of drying at 60 °C under vacuum. Finally, PU-HU_2-n (or PU-IPU_2-n) elastomers, boasting a thickness of 140 ± 13 μm, were achieved, free from any bubbles.

Characterization

The molecular structure of all products was determined by Fourier transform infrared (FTIR) spectroscopy and ^{1}H NMR spectroscopy. Fourier transform infrared (FTIR) spectra were acquired using a TENSOR II FT-IR spectrometer, employing the attenuated total reflectance (ATR) technique across the wavelength range of 650 - 4000 cm^{-1}. ^{1}H NMR spectra were recorded on a Bruker Advance II 400 MHz nuclear magnetic resonance spectrometer at room temperature. DMSO-d6 and $CDCl_3$ were utilized as solvents, with tetramethyl silane serving as the internal standard. Dynamic mechanical analysis (DMA) was conducted using a DMS 6100 dynamic mechanical analyzer, spanning a temperature range from -100 °C to 100 °C. The heating rate was set at 10 °C min^{-1}, with a sine wave oscillation frequency of 1 Hz. Wide-angle X-ray diffraction (WAXD) measurements were conducted using a Bruker D8 QUEST X-ray diffractometer, operating in continuous scanning mode with a Cu Kα X-ray generator (λ = 0.154 nm). To assess the microphase structure of the samples, tapping-mode

atomic force microscopy (AFM) was employed, utilizing a Demension icon Bruker system with an RTESPA-300 probe.

The tensile test was performed on the electronic universal testing machine (MTSMTS Criterion C42, 5 KN), employing a tensile rate of 50 mm min^{-1}. The tensile toughness of the sample was determined by integrating the area under the stress-strain curves. Additionally, cyclic tensile tests were conducted on the same machine, utilizing a tensile/recovered rate of 50 mm min^{-1}.

For the self-healing performance test, the film was initially scratched or cut using a blade. Subsequently, the healing process was examined. Surface observations of the damaged areas of the film were conducted using an Axiolab 5 ZEISS metalloscope. The mechanical properties of the healed film were evaluated through tensile test. The self-healing efficiency was calculated using the following formula:

$$\eta\ (\%) = \frac{\tau_{b_h}}{\tau_{b_i}} \times 100\% \quad \#(S1)$$

where η is the self-healing efficiency, τ_{b_h} and τ_{b_i} are tensile strength before and after healing, respectively.

The stress-relaxation experiment was conducted on a DMS 6100 dynamic mechanical analyzer, employing a strain control mode with a 10% strain. Subsequently, the relaxation modulus (G) was normalized by its initial value (G_0) to evaluate the material's relaxation behavior. The characteristic relaxation time (τ^*) was determined as the duration needed for G/G_0 to reach 1/e, which was achieved through the application of an exponential decay function:

$$G(t) = G_0 exp(-\frac{t}{\tau^*}) \#(S2)$$

The SAXS test was performed on a modified Xeuss system, utilizing a multilayer-focused Cu Kα X-ray source (GeniX3D Cu ULD, Xenocs SA, France; λ = 0.154 nm). The distance between the sample and detector was precisely maintained at 1185 nm. Subsequently, the one-dimensional SAXS data were thoroughly analyzed using the Fit2D software. The dimension (d) was accurately determined by applying Bragg's law:

$$d = \frac{2\pi}{q_{max}} \#(S3)$$

where q_{max} is the peak position of one-dimensional SAXA curve.

Transparency tests were conducted on a UV spectrometer (HITACHI U-3900) across a wavelength range of 400 nm to 800 nm, utilizing a medium scanning speed. The film utilized for these tests had a thickness of 120 μm.

Molecular dynamics (MD) simulations

Construction and simulation of the polyurethane elastomers

The Accelrys (BIOVIA) Materials Studio (MS) software was employed to build the simulation model and calculate key characteristic parameters. These parameters encompass the cohesive energy density (*CED*), visualization of the self-healing process, as well as the changes in hydrogen bond energy and vdW energy throughout the self-healing process. The Dreiding force field is chosen to comprehensively capture both intermolecular and intramolecular interactions throughout the simulation. The atomic equations of motion are meticulously solved using the Velocity Verlet algorithm. To ensure precision, a time integration step of 1 fs is set. To enhance

computational efficiency, nonbonded vdW interactions are truncated at a cutoff distance of 12.5 Å. For vdW interactions, atom-based summation methods are adopted to ensure the accurate of the calculations. Furthermore, strict criterion is established for the identification of hydrogen bonding. The length of the H-O bond is required to be less than 2.5 Å, and the angle of the O-H-N bond has to exceed 120°. These criteria are adopted to ensure an accurate representation of hydrogen bonding interactions within the simulation.

Four models were built, corresponding to the prepared PU-HU_2-n and PU-IPU_2-60. Each model consists of hard and soft segments in proportion to the prepared polyurethane. The initial configuration of the simulation system was constructed using the Amorphous Cell module to randomly distribute polymer chains within the simulation unit. Subsequently, an annealing process was conducted, consisting of one annealing cycle that included a linear heating process from 298 K to 798 K and a linear cooling process from 798 K to 298 K. The temperature was varied by a step of 100 K during both the heating and cooling process. The total simulation time for the annealing process was 5 ps, with a time step of 1 fs, under *NPT* ensemble at one bar pressure. After the annealing process, a dynamic process was performed under *NVT* ensemble conditions with a temperature of 298 K. The total simulation time for this process is 1 ps, with a time step of 1 fs.

Calculation of the cohesive energy density (*CED*)

The *CED* and CED_{vdW} can be directly obtained using the MD software. The CED_H however, requires a specific calculation. The cohesive energy of a system of molecules,

E_{coh}, represents the average energy required to separate all molecules to an infinite distance from each other. This cohesive energy is obtained by the following formula:

$$E_{coh} = - E_{inter} = E_{intra} - E_{total} \#(2)$$

where E_{inter} is the total intermolecular energy, E_{total} is the total energy of the system, and E_{intra} represents the intramolecular energy. Consequently, the E_{coh} of hydrogen bonds ($E_{coh\text{-}H}$) is obtain by subtracting the total energy of hydrogen bonds within each individual chain from the total energy of hydrogen bonds in the system. Subsequently, the cohesive energy density of hydrogen bond, CED_H, is simply the cohesive energy per unit of volume:

$$CED_H = \frac{E_{coh\text{-}H}}{V} \#(3)$$

where V is the cell volume.

Self-healing simulations and calculation

Initially, two computational cells designated as "A" and "B" were positioned within a box, separated by a 15 Å gap. Following geometry optimization, a dynamic process was initiated under *NVT* ensemble with a temperature set to 298 K. The total simulation time amounted to 2000 ps, with a time step of 1 fs. During the dynamic simulation, the vdW energy and hydrogen bond energy between "A" and "B" were meticulously calculated utilizing the following equations:

$$E_{inter}^{vdW} = E_{total}^{vdW} - E_{A}^{vdW} - E_{B}^{vdW} \#(4)$$

$$E_{inter}^{H} = E_{total}^{H} - E_{A}^{H} - E_{B}^{H} \#(5)$$

where the superscript "vdW" and "H" represent vdW energy and hydrogen bond energy, respectively. The subscripts "inter", "total", "A" and "B" refer to the corresponding parameter between "Part A" and "Part B', the entire system, "Part A" and "Part B", respectively.

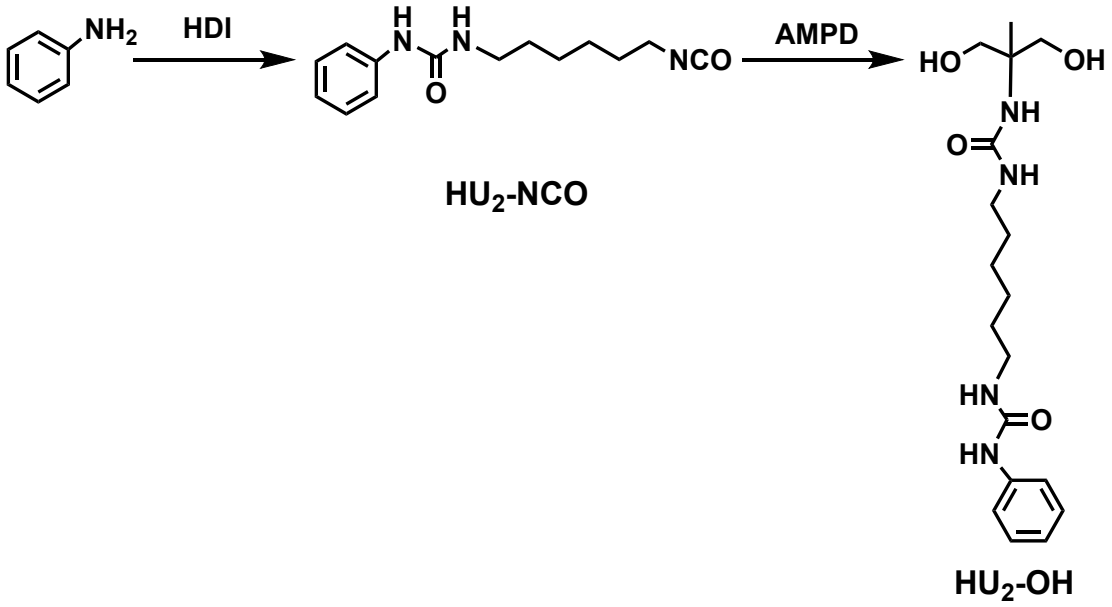

Fig. S1. Synthetic route of HU_2-NCO and HU_2-OH.

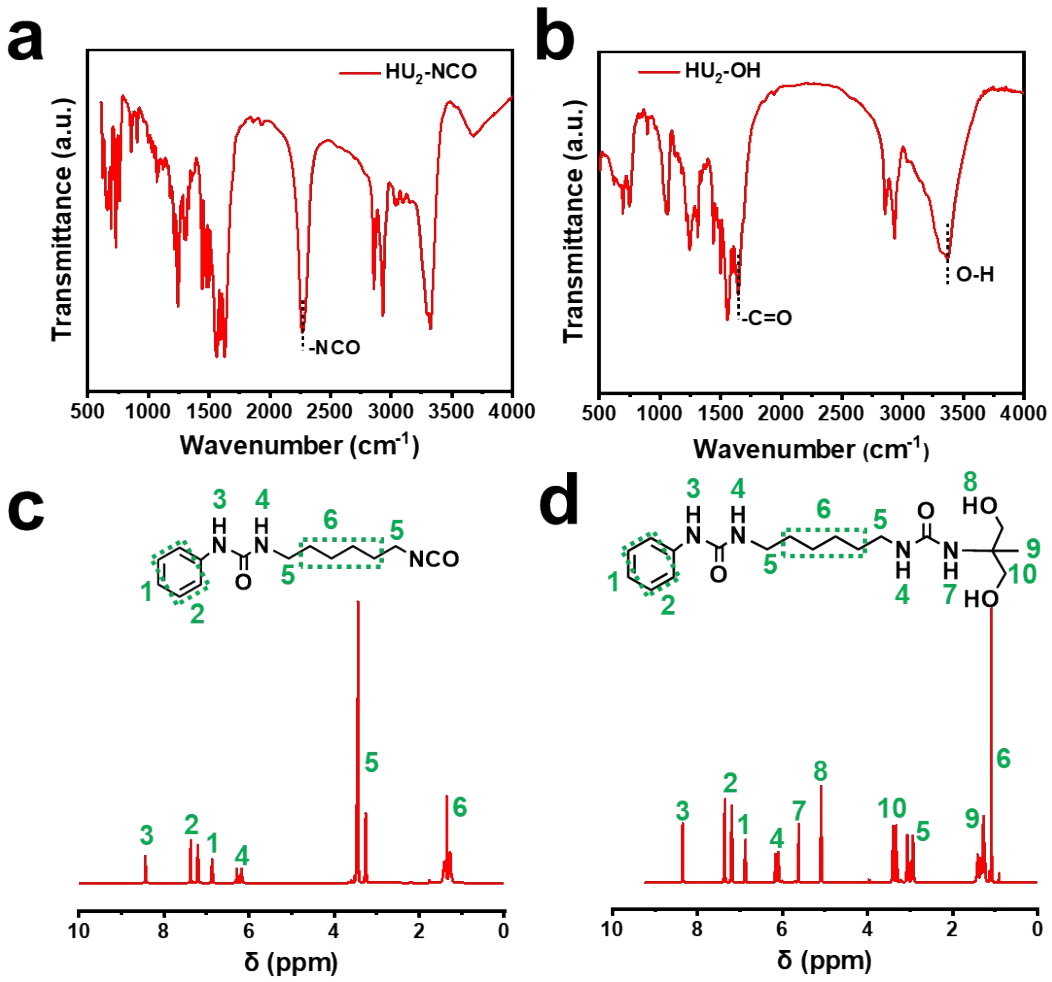

Fig. S2. Structural analysis of HU_2-NCO and HU_2-OH. (a) FT-IR spectra of HU_2-NCO and (b) HU_2-OH. The stretching vibration of the -NCO of HU_2-NCO is observed at 2270 cm^{-1}. In the case of HU_2-OH, the peak corresponding to -NCO disappears, and the stretching vibration of -C=O and O-H emerge at 1645 cm^{-1} and 3364 cm^{-1}, respectively. (c) ^1H NMR spectra of HU_2-NCO and (d) HU_2-OH.

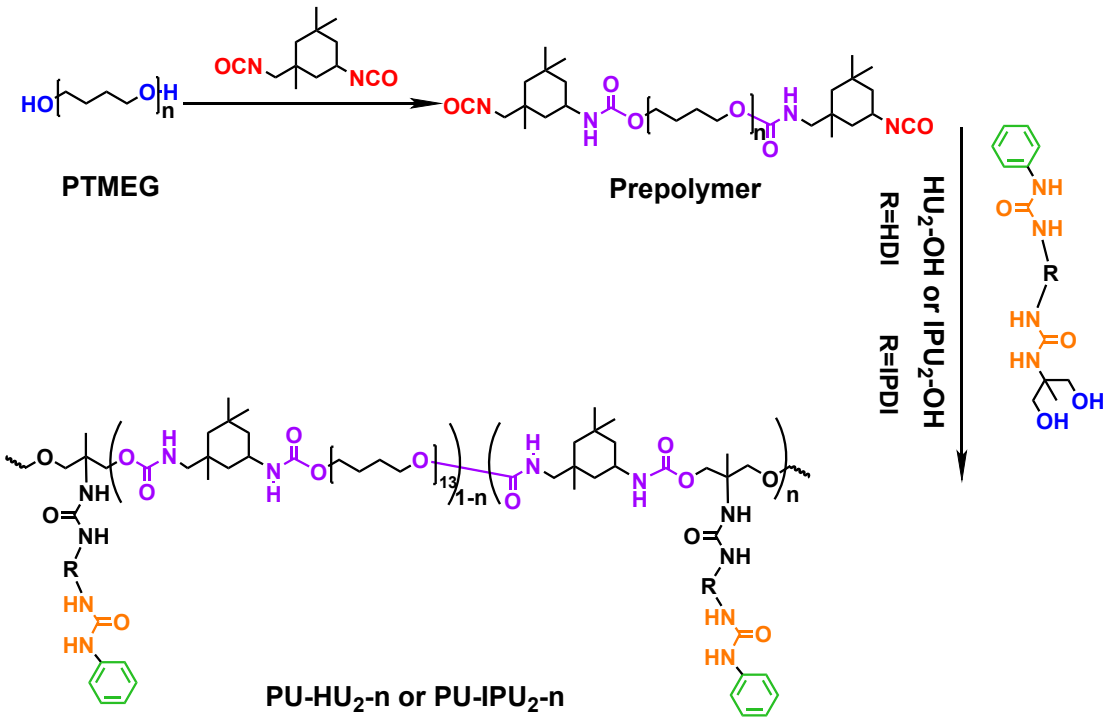

Fig. S3. Synthetic process of the prepared elastomers.

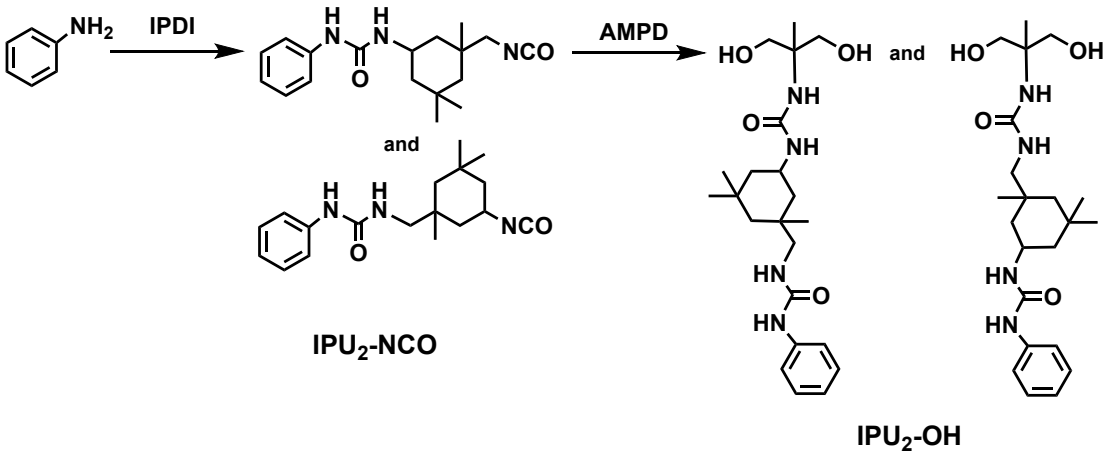

Fig. S4. Synthetic route of IPU_2-NCO and IPU_2-OH.

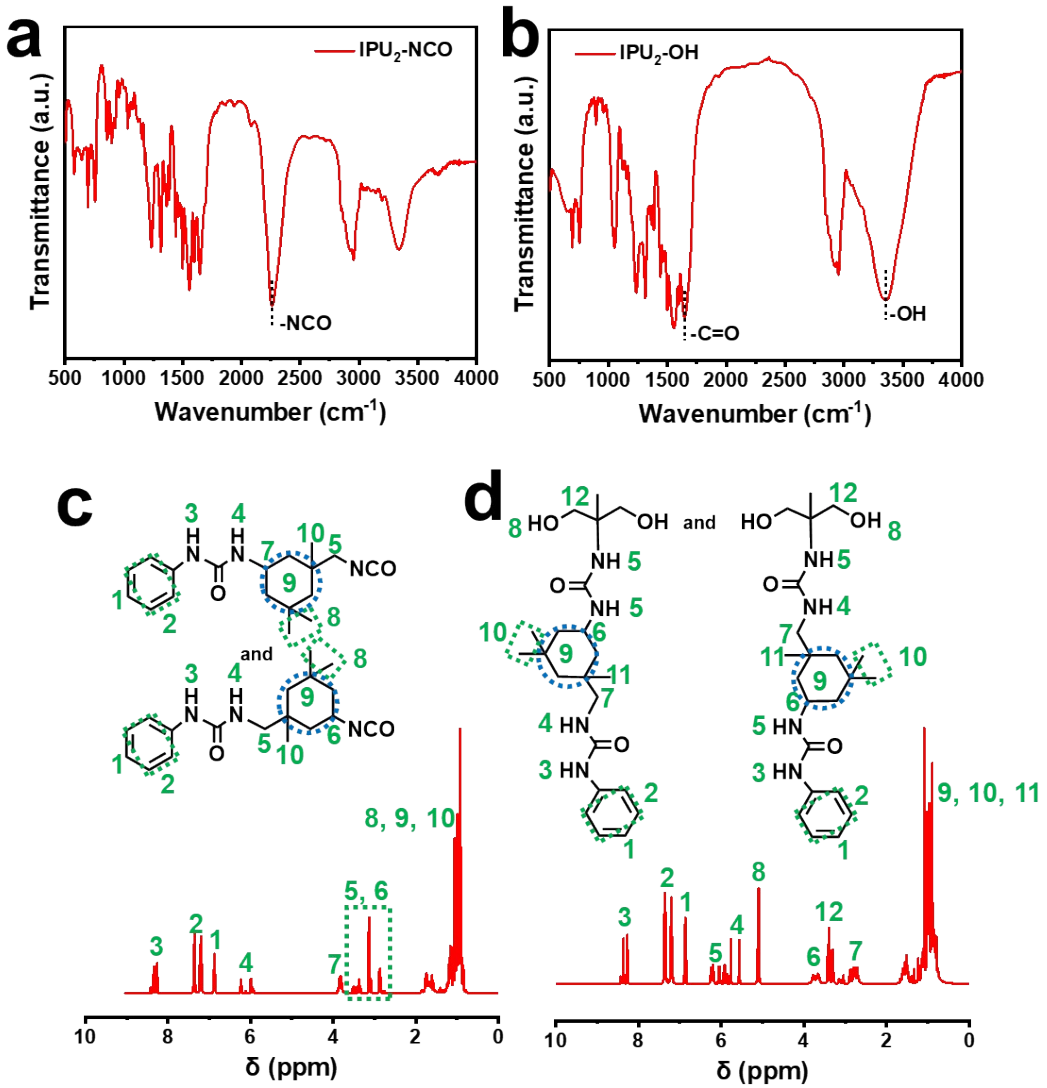

Fig. S5. Structural analysis of IPU_2-NCO and IPU_2-OH. (a) FT-IR spectra of IPU_2-NCO and (b) IPU_2-OH. (c) ^1H NMR spectra of IPU_2-NCO and (d) IPU_2-OH.

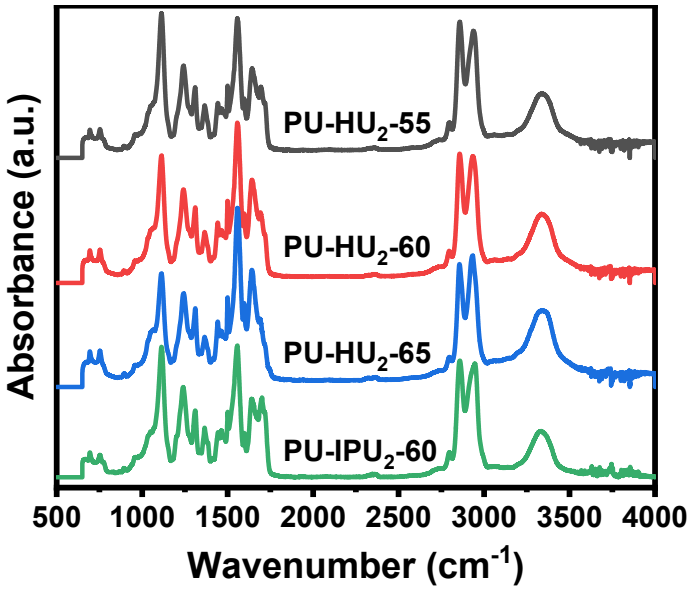

Fig. S6. FTIR spectra of the prepared elastomers.

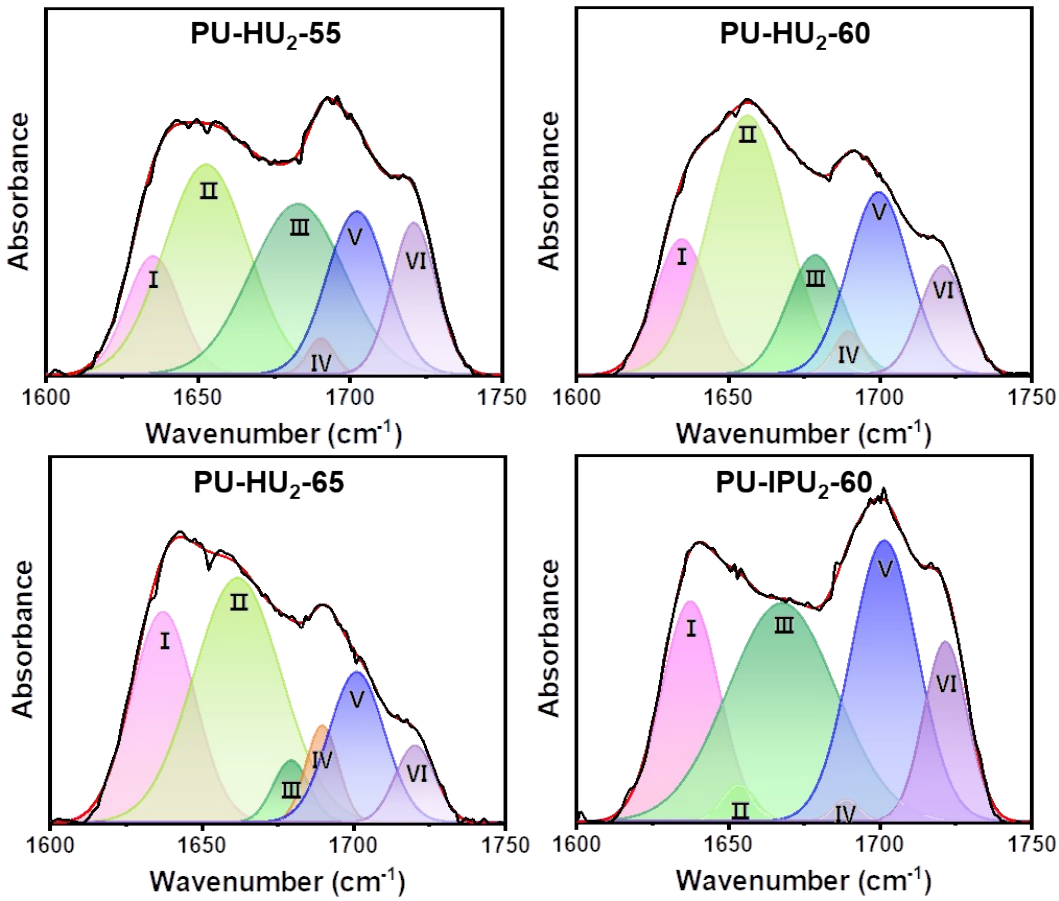

Fig. S7. Peak-splitting fitting diagram of C=O infrared peaks.

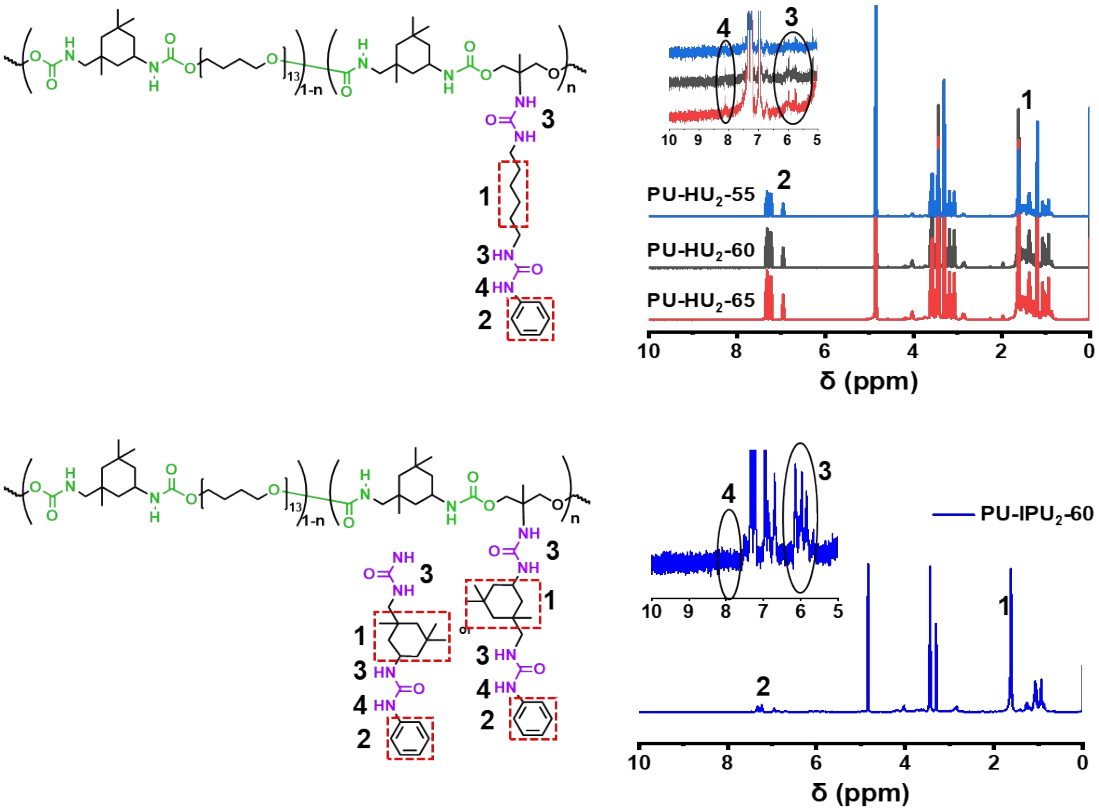

Fig. S8. ^{1}H NMR spectra of PU-HU$_2$-n and PU-IPU$_2$-60.

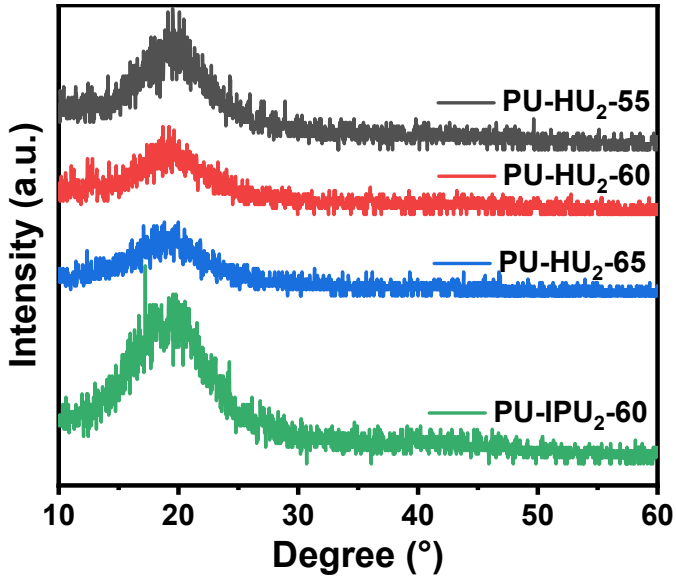

Fig. S9. The WAXD spectra of the prepared elastomers.

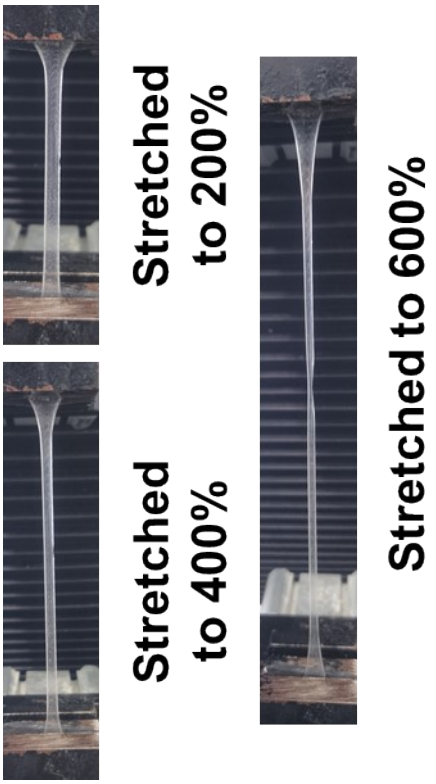

Fig. S10. Photographs of the notched PU-HU_2-65 sample with different strains during the stretching process.

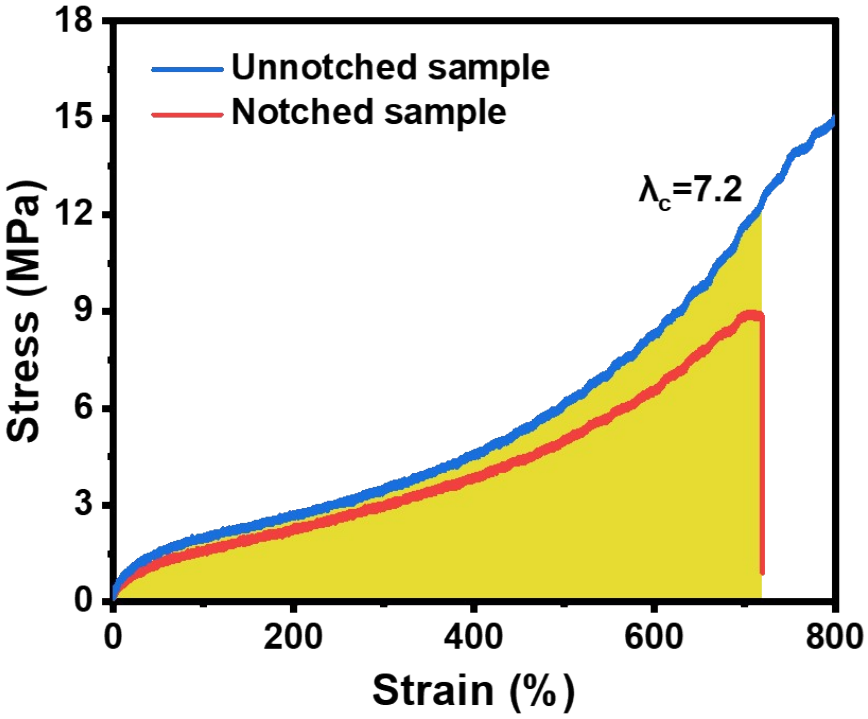

Fig. S11. Typical stress-strain curves of the unnotched and notched PU-HU_2-65 sample.

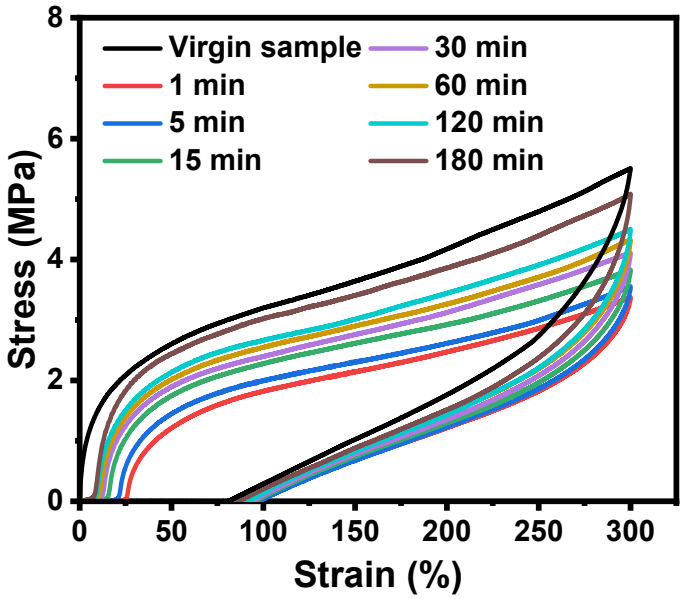

Fig. S12. Cyclic tensile curves of PU-HU_2-65 sample after recover for different times.

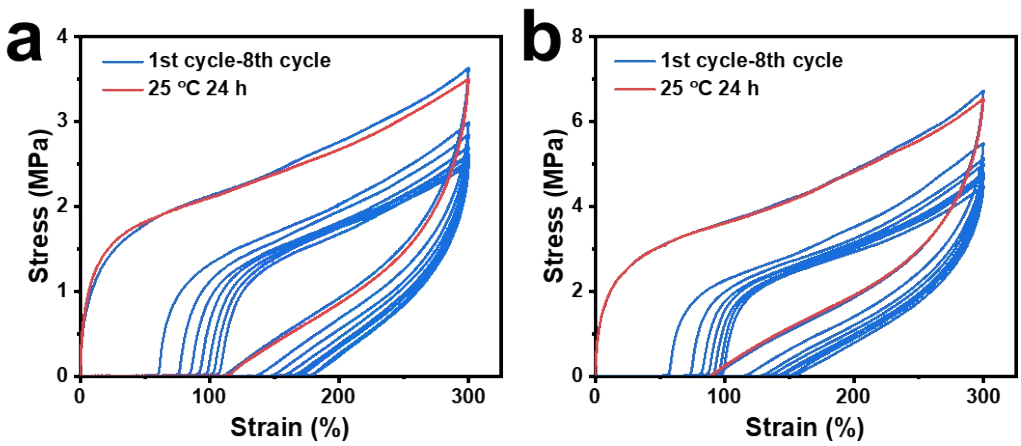

Fig. S13. Consecutive cyclic tensile curves of PU-HU_2-60 and PU-HU_2-65 elastomers with a strain of 300%.

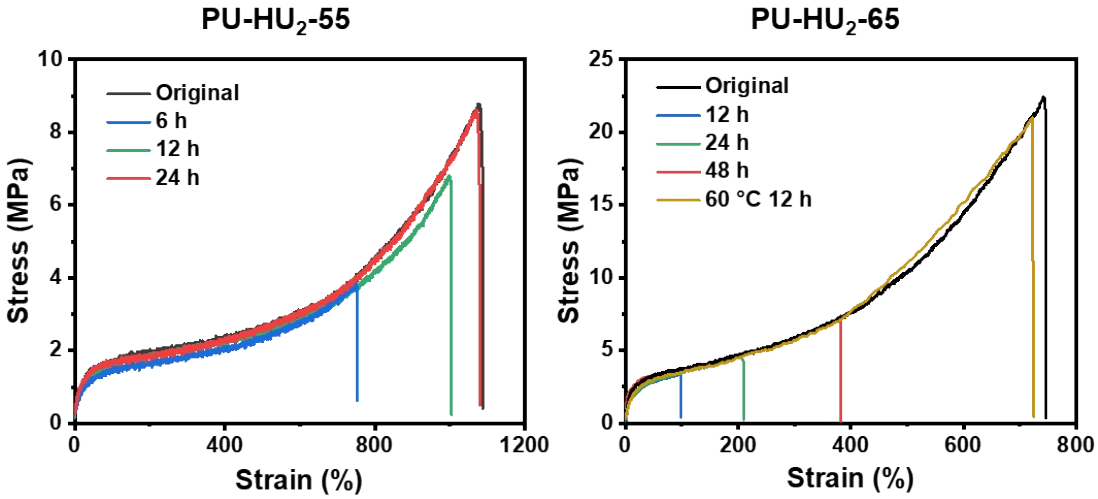

Fig. S14. Typical tensile curves of the healed PU-HU_2-55 and PU-HU_2-65 samples.

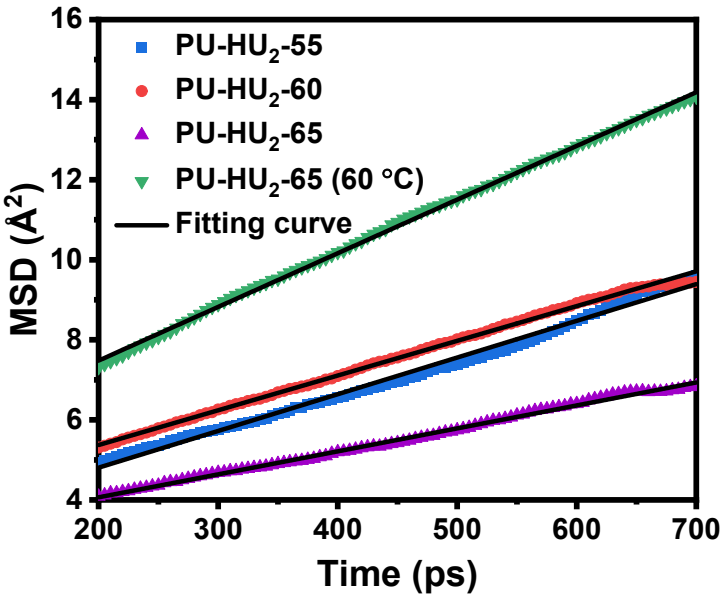

Fig. S15. MSD of PU-HU_2-n elastomers at different times.

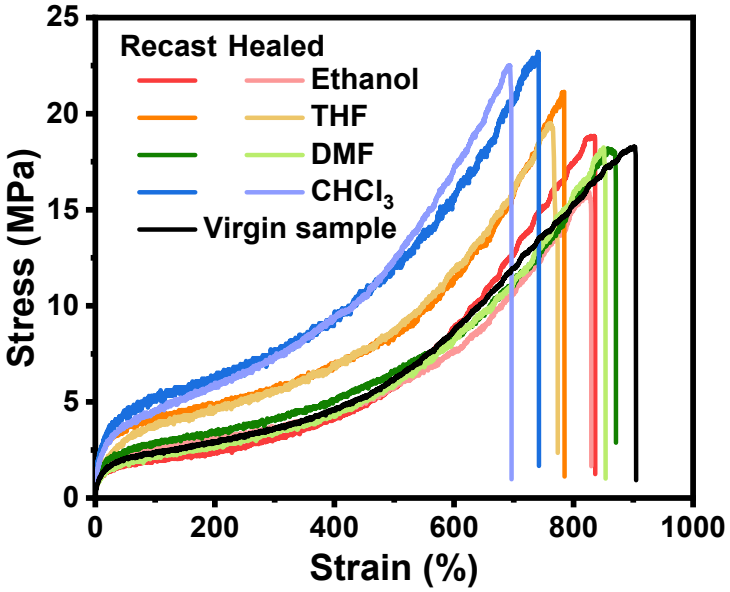

Fig. S16. Tensile curves of the recast and recast-repaired PU-HU_2-60 elastomer.

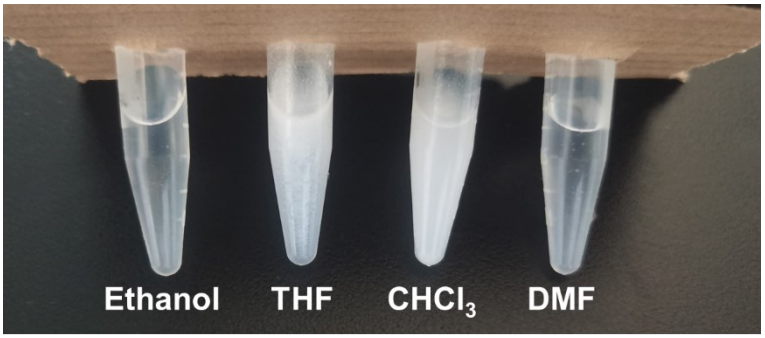

Fig. S17. Photographs of HU_2-OH dissolved in different organic solvents.

Table S1. Summary of the assignment of the deconvoluted subpeaks in the FTIR C=O absorption bands for the prepared elastomers.

Assignment		Wavenumber (cm^{-1})				Area (%)			
		PU-HU_2-55	PU-HU_2-60	PU-HU_2-65	PU-IPU_2-60	PU-HU_2-55	PU-HU_2-60	PU-HU_2-65	PU-IPU_2-60
ν (C=O) urea	I (Ordered H-bonded)	1635	1635	1637	1639	10.98	14.05	25.84	23.37
	II (Disordered H-bonded)	1652	1657	1662	1654	30.78	39.17	41.57	1.29
	III (free)	1682	1679	1680	1669	27.73	13.01	4.28	32.35
ν (C=O) urethane	IV (Ordered H-bonded)	1690	1690	1690	1685	1.67	2.43	6.09	0.20
	V (Disordered H-bonded)	1702	1699	1701	1700	17.06	21.69	16.25	32.91
	VI (free)	1721	1721	1720	1721	11.78	9.65	5.97	9.88

Table S2. Summary of the mechanical parameters of the prepared elastomers.

Elastomer	Tensile strength (MPa)	Ultimate elongation (%)	Toughness (MJ m^{-3})
PU-HU_2-55	8.79±0.96	1023.3±165.8	38.45±1.07
PU-HU_2-60	18.27±2.21	904.6±68.5	66.10±1.68
PU-HU_2-65	22.35±1.96	745.8±86.5	66.86±0.96
PU-IPU_2-60	12.71±1.65	108.5±6.4	12.01±0.12

Table S3. Summary of the mechanical parameters of the healed PU-HU_2-55 elastomer.

Healing time (h)	Tensile strength (MPa)	Ultimate elongation (%)	Toughness (MJ m^{-3})
6	3.84±0.62	752.5±56.9	16.01±0.41
12	6.81±1.32	1004±102.3	29.18±1.19
24	8.62±1.24	1079.6±78.6	37.37±0.73

Table S4. Summary of the mechanical parameters of the healed PU-HU_2-60 elastomer.

Healing time (h)	Tensile strength (MPa)	Ultimate elongation (%)	Toughness (MJ m^{-3})
12	3.93±0.24	329.4±20.6	9.76±0.27
24	9.41±0.75	625±73.2	30.12±1.62
36	17.62±0.84	890.8±56.8	60.89±1.57

Table S5. Summary of the mechanical parameters of the healed PU-HU_2-65 elastomer.

Healing time (h)	Tensile strength (MPa)	Ultimate elongation (%)	Toughness (MJ m^{-3})
12	3.5±0.18	98.4±7.2	2.17±0.03
24	4.65±0.41	209.6±16.5	7.35±0.15
48	7.03±0.46	381.1±22.7	16.75±0.64
12 (60 °C)	20.99±1.25	724.4±86.5	62.86±1.93